

# Facile labelling of an anti-epidermal growth factor receptor Nanobody with $^{68}\text{Ga}$ via a novel bifunctional desferal chelate for immuno-PET

Maria J. W. D. Vosjan · Lars R. Perk · Rob C. Roovers · Gerard W. M. Visser ·  
Marijke Stigter-van Walsum · Paul M. P. van Bergen en Henegouwen ·  
Guus A. M. S. van Dongen

Received: 10 August 2010 / Accepted: 29 November 2010 / Published online: 6 January 2011  
© The Author(s) 2010. This article is published with open access at Springerlink.com

## Abstract

**Purpose** The ~15 kDa variable domains of camelid heavy-chain-only antibodies (called Nanobodies®) have the flexibility to be formatted as monovalent, monospecific, multivalent or multispecific single chain proteins with either fast or slow pharmacokinetics. We report the evaluation of the fast kinetic anti-epidermal growth factor receptor (EGFR) Nanobody 7D12, labelled with  $^{68}\text{Ga}$  via the novel bifunctional chelate (BFC) *p*-isothiocyanatobenzyl-desferrioxamine (Df-Bz-NCS). Df-Bz-NCS has recently been introduced as the chelate of choice for  $^{89}\text{Zr}$  immuno-positron emission tomography (PET).

**Methods** Nanobody 7D12 was premodified with Df-Bz-NCS at pH 9. Radiolabelling with purified  $^{68}\text{Ga}$  was performed at pH 5.0–6.5 for 5 min at room temperature. For in vitro stability measurements in storage buffer (0.25 M NaOAc with

5 mg ml<sup>-1</sup> gentisic acid, pH 5.5) at 4°C or in human serum at 37°C, a mixture of  $^{67}\text{Ga}$  and  $^{68}\text{Ga}$  was used. Biodistribution and immuno-PET studies of  $^{68}\text{Ga}$ -Df-Bz-NCS-7D12 were performed in nude mice bearing A431 xenografts using  $^{89}\text{Zr}$ -Df-Bz-NCS-7D12 as the reference conjugate.

**Results** The Df-Bz-NCS chelate was conjugated to Nanobody 7D12 with a chelate to Nanobody molar substitution ratio of 0.2:1. The overall  $^{68}\text{Ga}$  radiochemical yield was 55–70% (not corrected for decay); specific activity was 100–500 MBq/mg. Radiochemical purity of the conjugate was >96%, while the integrity and immunoreactivity were preserved.  $^{68/67}\text{Ga}$ -Df-Bz-NCS-7D12 was stable in storage buffer as well as in human serum during a 5-h incubation period (<2% radioactivity loss). In biodistribution studies the  $^{68}\text{Ga}$ -labelled Nanobody 7D12 showed high uptake in A431 tumours (ranging from 6.1±1.3 to 7.2±1.5%ID/g at 1–3 h after injection) and high tumour to blood ratios, which increased from 8.2 to 14.4 and 25.7 at 1, 2 and 3 h after injection, respectively. High uptake was also observed in the kidneys. Biodistribution was similar to that of the reference conjugate  $^{89}\text{Zr}$ -Df-Bz-NCS-7D12. Tumours were clearly visualized in a PET imaging study.

**Conclusion** Via a rapid procedure under mild conditions a  $^{68}\text{Ga}$ -Nanobody was obtained that exhibited high tumour uptake and tumour to normal tissue ratios in nude mice bearing A431 xenografts. Fast kinetic  $^{68}\text{Ga}$ -Nanobody conjugates can be promising tools for tumour detection and imaging of target expression.

M. J. W. D. Vosjan · L. R. Perk · M. Stigter-van Walsum ·  
G. A. M. S. van Dongen (✉)  
Department of Otolaryngology/Head and Neck Surgery,  
VU University Medical Center,  
De Boelelaan 1117, P.O. Box 7057, 1007 MB Amsterdam,  
The Netherlands  
e-mail: gams.vandongen@vumc.nl

G. W. M. Visser · G. A. M. S. van Dongen  
Department of Nuclear Medicine & PET Research,  
VU University Medical Center,  
Amsterdam, The Netherlands

R. C. Roovers · P. M. P. van Bergen en Henegouwen  
Cellular Dynamics, Science Faculty, Utrecht University,  
Utrecht, The Netherlands

**Keywords**  $^{68}\text{Ga}$  · Radiolabelling · Nanobodies · Desferal ·  
*p*-Isothiocyanatobenzyl-desferrioxamine · EGFR

## Introduction

The epidermal growth factor receptor (EGFR, HER1, ERb1) is a transmembrane protein of the tyrosine kinase receptor family. Activation of EGFR causes signalling that may lead to cell division, increased motility, angiogenesis and suppression of apoptosis [1]. EGFR over-expression or constitutive activation has been shown to be associated with poor survival and recurrences in many human malignancies [2]. Detection of EGFR expression via nuclear medicine visualization may provide advantages over immunohistochemical staining of tumour biopsies, since evaluation of both the primary tumour as well as the metastases can be achieved. In addition, such confirmation of EGFR expression can be of value as a scouting procedure to select patients for anti-EGFR therapy with approved monoclonal antibodies (mAbs) like cetuximab or panitumumab or small molecular tyrosine kinase inhibitors. On this latter topic several studies with intact anti-EGFR ( $\alpha$ EGFR) mAbs or mAb fragments labelled with single photon emission computed tomography (SPECT) ( $^{111}\text{In}$ ,  $^{99\text{m}}\text{Tc}$ ) or positron emission tomography (PET) ( $^{64}\text{Cu}$ ,  $^{89}\text{Zr}$ ) radionuclides have been reported [3–9].

Nanobody technology provides new perspectives for mono- as well as multitarget tumour detection and therapy [10–12]. Nanobodies are derived from a unique antibody format that is present in species from the family of *Camelidae*, including llama, camel and dromedary. These animals contain, besides their conventional antibody repertoire, an antibody class consisting of heavy chains only [10, 13]. The variable region of the heavy-chain-only antibodies (VHH) represents the complete binding unit of the antibody. Because of the small size of these VHH fragments (~15 kDa), this binding unit is also called Nanobody®. Although being smaller than a scFv fragment, a Nanobody has full antigen-binding potential and does not show aggregation problems, because of hydrophilic instead of hydrophobic patches in the  $V_{\text{H}}$  and  $V_{\text{L}}$  domains. Due to their single domain character, standard molecular biology techniques such as polymerase chain reaction (PCR) allow for the facile purification and selection of appropriate Nanobody candidates from the full antibody repertoire of immunized animals [14]. Unique features of the Nanobody technology platform in comparison to conventional mAb technology are easy and rapid drug development, and the easy and cheap production in bacteria and yeast [10, 15].

For a proof of concept we used the Nanobody technology platform to construct two  $\alpha$ EGFR Nanobodies [11]. The biodistribution of a  $^{177}\text{Lu}$ -labelled bivalent  $\alpha$ EGFR Nanobody ( $\alpha$ EGFR- $\alpha$ EGFR) in A431 tumour-bearing nude mice showed a tumour uptake of  $5.0 \pm 1.4$

percentage of the injected dose per gram of tissue (%ID/g) at 6 h after injection and high tumour to normal tissue ratios (e.g. tumour to blood ratio >80) due to rapid blood clearance. Simple fusion of an anti-albumin Nanobody building block gave a 50-kDa single-chain construct ( $\alpha$ EGFR- $\alpha$ EGFR- $\alpha$ Alb) that showed pharmacokinetics and tumour uptake (up to  $35.2 \pm 7.5\%$  ID/g) comparable to cetuximab, but faster and deeper tumour penetration. Therefore, such Nanobody formats might be ideal for imaging and therapeutic purposes, respectively.

In the present study we evaluated the in vivo diagnostic potential of fast kinetic  $\alpha$ EGFR Nanobody 7D12 with the immuno-PET approach. For this purpose the short-lived positron emitter  $^{68}\text{Ga}$  ( $T_{1/2}=68$  min,  $E_{\beta+\text{max}}$  1.92 MeV) was chosen.  $^{68}\text{Ga}$  is an attractive positron-emitting radionuclide since it is cyclotron-independently available via the  $^{68}\text{Ge}/^{68}\text{Ga}$  generator system.

In aqueous solutions the three-valent gallium forms a complex with many bifunctional chelates (BFCs) containing oxygen and nitrogen as donor atoms. The only clinically used BFC for  $^{68}\text{Ga}$  is 1,4,7,10-tetraazacyclododecane-*N,N',N'',N'''*-tetraacetic acid (DOTA), but fast complex formation requires a high temperature [16–19]. More recently, several new chelates have been described for labelling of  $^{68}\text{Ga}$  to heat-labile proteins at ambient temperature including 1,4,7-triazacyclononane-1,4,7-triacetic acid (NOTA) and *N,N'*-bis[2-hydroxy-5-(carboxyethyl)benzyl]ethylenediamine-*N,N'*-diacetic acid (HBED-CC) [19–21]. However, this new generation of BFCs is not yet available for clinical immuno-PET applications.

For coupling of the long-lived positron emitter  $^{89}\text{Zr}$  ( $T_{1/2}=78.4$  h,  $E_{\beta+\text{max}}$  0.9 MeV) (23%) to intact mAbs, we recently introduced the novel BFC *p*-isothiocyanatobenzyl derivative of desferrioxamine B (Df-Bz-NCS) [22, 23]. The choice of desferrioxamine B is attractive because it has been used safely in the clinical setting for many years. Since the hydroxamate function in desferrioxamine B has also been used for coupling of  $^{67}\text{Ga}$  in the past [24–27], we investigated whether this same Df-Bz-NCS can be used for labelling of  $^{68}\text{Ga}$  under mild conditions. If so, a similar kind of GMP-compliant radiochemistry can be used for labelling of slow kinetic mAbs with  $^{89}\text{Zr}$ , and fast kinetic mAb fragments with  $^{68}\text{Ga}$ .

In this study, after establishing optimal  $^{68}\text{Ga}$  labelling procedures by using a control intact IgG mAb, the bifunctional chelate Df-Bz-NCS was conjugated to  $\alpha$ EGFR Nanobody 7D12 and subsequently radiolabelled with  $^{68}\text{Ga}$ . The resulting  $^{68}\text{Ga}$ -Df-Bz-NCS-7D12 conjugate was analysed for stability at 4°C in storage buffer and at 37°C in serum, whereas its in vivo behaviour was investigated via biodistribution and animal PET studies, using  $^{89}\text{Zr}$ -Df-Bz-NCS-7D12 as the reference.

## Materials and methods

### Materials

All reagents were purchased from Sigma-Aldrich (St. Louis, MO, USA) unless otherwise stated. Deionized water (18 M $\Omega$ \*cm) and ultra pure HCl (Ga content 0.02 ng <sup>nat</sup>Ga/g) was used. No other special measures were taken regarding working under strict metal-free conditions. Df-Bz-NCS was purchased from Macrocyclics (Dallas, TX, USA, catalog No. B-705). Nanobody 7D12 was generated by Ablynx NV (Ghent, Belgium) as described previously [14] and kindly provided to us. The selection, production and characterization of chimeric mAb U36 (cmAb U36 11.53 mg/ml) directed against CD44v6 has been described elsewhere [28]. The human epidermoid cervical carcinoma cell line A431 was obtained from the American Type Culture Collection ([www.atcc.com](http://www.atcc.com)), ATCC number: CRL-1555. The head and neck squamous cell carcinoma (HNSCC) cell line UM-SCC-11B was obtained from Dr. T.E. Carey (Ann Arbor, MI, USA) [29]. <sup>68</sup>Ga was obtained from a commercial <sup>68</sup>Ge/<sup>68</sup>Ga generator based on a TiO<sub>2</sub> bedding with 1.85 GBq <sup>68</sup>Ge-loaded activity (IGG100; Eckert & Ziegler, Berlin, Germany). <sup>67</sup>Ga was purchased as <sup>67</sup>Ga-citrate (74 MBq/ml) from Covidien (Mansfield, MA, USA). [<sup>89</sup>Zr]Zr-oxalate in 1.0 M oxalic acid ( $\geq 0.15$  GBq/nmol) was from IBA Molecular ([www.iba.be/molecular](http://www.iba.be/molecular)).

### Purification and concentration of <sup>68</sup>Ga and <sup>67</sup>Ga

The <sup>68</sup>Ga was eluted from the <sup>68</sup>Ge/<sup>68</sup>Ga generator as described by Velikyan et al. [16]. In short, the generator was eluted according to the manufacturer's protocol with 3.5 ml ultra pure 0.1 M HCl solution. To that solution 3.5 ml ultra pure 8 M HCl was added under stirring, to give a final concentration of  $\sim 4$  M HCl. The solution was passed through a pre-treated (1 ml 100% ethanol, 1 ml deionized water, 1 ml 4 M HCl) anion exchange column [Chromafix, PS-HCO<sub>3</sub> (s), Macherey-Nagel, Düren, Germany], the column was washed with 2 ml of 4 M HCl, flushed with air, and then the <sup>68</sup>Ga was eluted from the Chromafix column with 200  $\mu$ l deionized water (elution efficiency  $>85\%$ ). The use of ultra pure HCl implies that this procedure attributes at most 1.1 pmol <sup>nat</sup>Ga to this eluate.

<sup>67</sup>GaCl<sub>3</sub> was obtained from <sup>67</sup>Ga-citrate. To this end, <sup>67</sup>Ga-citrate was mixed with an equal volume of ultra pure 8 M HCl. This solution was passed through a pre-treated Chromafix column and eluted as described for <sup>68</sup>Ga.

In all preparations for in vitro evaluation <sup>68/67</sup>Ga was used, while for in vivo evaluation only <sup>68</sup>Ga was applied.

### Preparation of <sup>68/67</sup>Ga-Df-Bz-NCS-cmAb U36

For development of labelling procedures, the 150-kDa intact cmAb U36 was used as the control mAb. cmAb U36 was premodified with Df-Bz-NCS as described by Perk et al. [22] (Fig. 1). In short, 5 mg cmAb U36 (33 nmol) reacted with 20  $\mu$ l Df-Bz-NCS (100 nmol) in dimethyl sulphoxide (DMSO) for 30 min at 37°C at pH 9 in a shaker, in a total volume of 1 ml. Nonconjugated chelate was removed by size exclusion chromatography using a PD-10 column (GE Healthcare Life Science) with 0.25 M NaOAc pH 5.5 as eluant. The flow through and the first 1.5 ml were discarded. The next 2 ml containing the premodified mAb were stored.

Ga-Df complex chelate formation conditions were selected by varying pH and protein concentration. As a result, the following procedure was developed; to 10–200  $\mu$ l (=a) <sup>68</sup>Ga and/or <sup>67</sup>Ga in deionized water ( $3 \times a$   $\mu$ l), 3 M NH<sub>4</sub>OAc buffer pH 7.2 were added and mixed for 5 min at room temperature. Subsequently the premodified cmAb U36 (100–1,000  $\mu$ g) in 0.25 M NaOAc pH 5.5 was added; the final reaction volume was 2 ml. The reaction was stopped after 5 min at room temperature by the addition of 50  $\mu$ l 50 mM ethylenediaminetetraacetate acid (EDTA), followed by PD-10 column purification using 0.25 M NaOAc with 5 mg ml<sup>-1</sup> gentisic acid, pH 5.5, as eluant. The flow through and the first 1 ml were discarded. The next 2 ml containing the <sup>68/67</sup>Ga-labelled cmAb U36 was collected and used for further experiments.

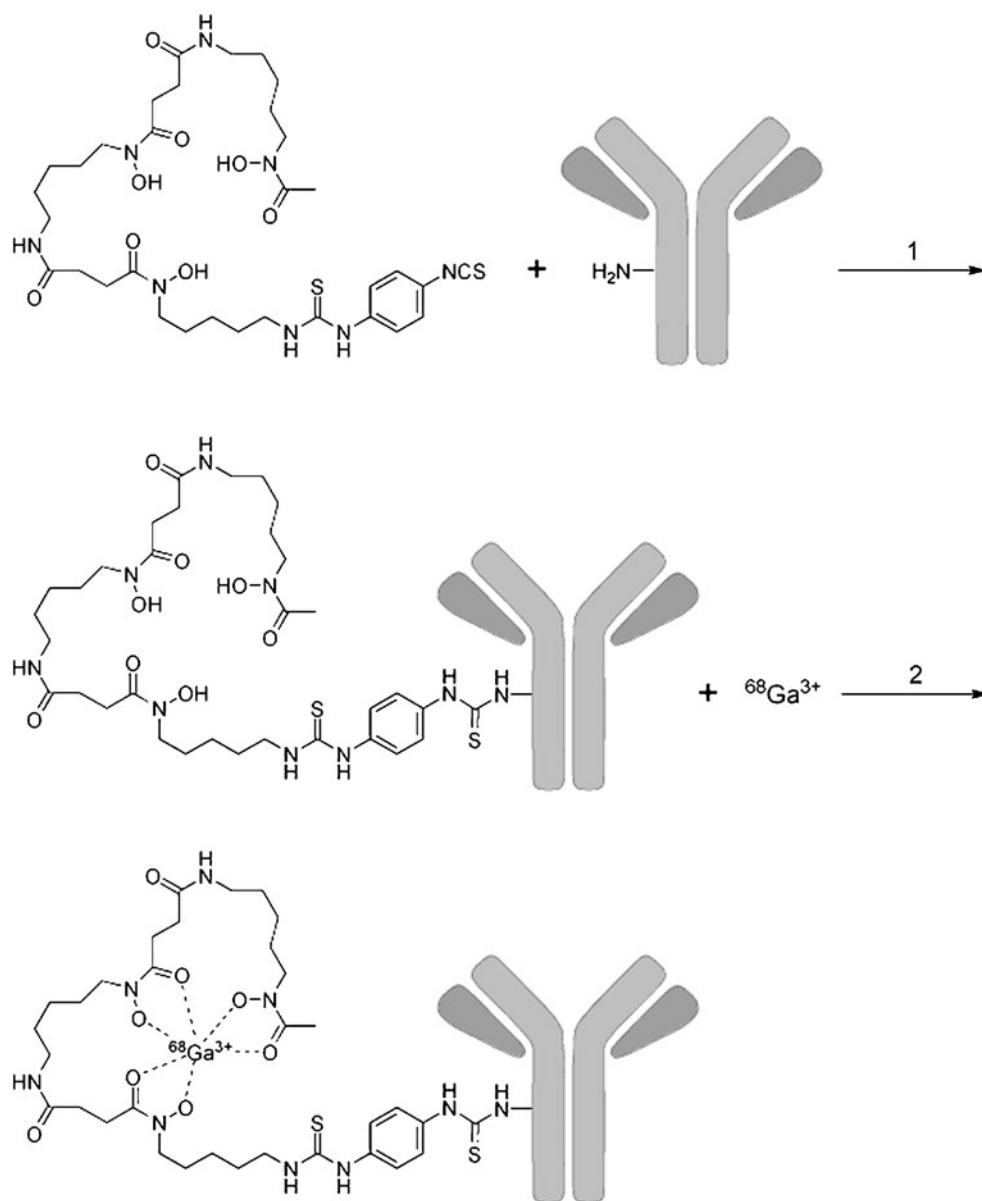
### Preparation of <sup>68/67</sup>Ga-Df-Bz-NCS-7D12

The same protocol was applied for the modification and radiolabelling of the  $\alpha$ EGFR Nanobody 7D12. In short, 2 mg 7D12 (125 nmol) was conjugated with 375 nmol Df-Bz-NCS and after PD-10 column purification the premodified 7D12 (200–1,000  $\mu$ g) was labelled with <sup>68/67</sup>Ga as described for cmAb U36.

### Preparation of <sup>89</sup>Zr-Df-Bz-NCS-7D12

The 7D12 nanobody was premodified as described above with a threefold molar excess of Df-Bz-NCS chelate. After PD-10 column purification the premodified 7D12 was labelled with <sup>89</sup>Zr as described by Perk et al. [22]. In short, Df-Bz-NCS-7D12 (100–1,000  $\mu$ g) was labelled with <sup>89</sup>Zr (37 MBq) in 0.25 M HEPES buffer pH 7.0 at room temperature in a total volume of 2 ml. The <sup>89</sup>Zr-Df-Bz-NCS-7D12 was purified by PD-10 column using 0.25 M NaOAc with 5 mg ml<sup>-1</sup> gentisic acid, pH 5.5, as eluant. After discarding the flow through and the first 1 ml, the next 2 ml containing the <sup>89</sup>Zr-labelled 7D12 was collected for further experiments.

**Fig. 1** Two-step synthesis of  $^{68}\text{Ga}$ -Df-Bz-NCS-mAb with the bifunctional chelate Df-Bz-NCS



#### Determination of Df to 7D12 molar ratio

The Df-Bz-NCS to 7D12 molar ratio was determined following a general method using a known nanomolar excess of  $\text{GaCl}_3$  spiked with  $^{67}\text{Ga}$ . In short, 250 nmol  $\text{GaCl}_3$  (in 4 M ultra pure HCl) was mixed with  $\sim 37$  MBq  $^{67}\text{Ga}$  and purified according to the aforementioned method using the anion Chromafix column. Thereafter, 500  $\mu\text{g}$  of premodified Df-Bz-NCS-7D12 was labelled according to the developed protocol with 20–60 nmol of the above prepared  $^{67}\text{Ga}$ - $\text{GaCl}_3$ , and the Df to 7D12 molar ratio was calculated. For comparison the Df to 7D12 molar ratio was also determined with the use of zirconium oxalate spiked with  $^{89}\text{Zr}$ .

#### Analysis

$^{68}\text{Ga}$  was measured using  $E_\gamma = 511$  KeV and  $^{67}\text{Ga}$  with  $E_\gamma = 185$  KeV. When dual isotope labelling products were produced,  $^{67}\text{Ga}$  radioactivity measurements were performed at least 20 h after production (after decay of  $^{68}\text{Ga}$ ). Each  $^{68}/^{67}\text{Ga}$ -labelled product was analysed by instant thin-layer chromatography (ITLC) to determine the radiochemical labelling efficiency and radiochemical purity. The integrity of the Nanobody and mAb was analysed by high-performance liquid chromatography (HPLC) and sodium dodecyl sulphate polyacrylamide gel electrophoresis (SDS-PAGE) followed by phosphor imaging (Storm 820, GE Healthcare). Immunoreactivity was determined by a cell-

binding assay, 3 h at 37°C or overnight at 4°C. ITLC analysis of the  $^{68/67}\text{Ga}$ -labelled products was performed on chromatography strips (Biodex, Shirley, NY, USA); 2  $\mu\text{l}$  was spotted on an ITLC strip with 50 mM EDTA in Milli-Q as mobile phase. HPLC analysis was performed on a Jasco HPLC system using a Superdex™ peptide size exclusion column (GE Healthcare Life Sciences) when a labelled Nanobody was injected, or a Superdex™ 200 10/300 GL size exclusion column when labelled cmAb U36 was injected, with a mixture of 0.05 M sodium phosphate and 0.15 M sodium chloride (pH 6.8) as eluant at flow rates of 1.0 and 0.5  $\text{ml min}^{-1}$ , respectively. Gel electrophoresis was performed on a PhastGel System (GE Healthcare Life Sciences) using high-density SDS-PAGE gels when a labelled Nanobody was applied or 7.5% SDS-PAGE gels when labelled U36 was applied, under non-reducing conditions. Immunoreactivity was determined by measuring the binding of the  $^{68/67}\text{Ga}$ -7D12 or  $^{68/67}\text{Ga}$ -cmAb U36 to a serial dilution of 2% paraformaldehyde fixed A431 cells or 0.2% glutaraldehyde fixed 11B cells, respectively, essentially as described by Lindmo et al. [30].

#### In vitro stability

To determine the in vitro stability of the gallium-labelled Nanobodies, 500  $\mu\text{g}$   $^{68/67}\text{Ga}$ -labelled 7D12 product was stored at 4°C up to 24 h in 0.25 M NaOAc pH 5.5, containing 5  $\text{mg ml}^{-1}$  gentisic acid as antioxidant and compared with  $^{89}\text{Zr}$ -7D12. Amounts of activity at the start of storage were 120 MBq of  $^{68}\text{Ga}$ , 20 MBq of  $^{67}\text{Ga}$  and 20 MBq of  $^{89}\text{Zr}$ . After 5 and 24 h storage aliquots were taken and analysed by ITLC, HPLC and SDS-PAGE.

Stability of  $^{68/67}\text{Ga}$ -labelled 7D12 was also tested in freshly prepared human serum and compared with  $^{89}\text{Zr}$ -7D12. Activity amounts at the start of storage were 80 MBq  $^{68}\text{Ga}$ , 18 MBq  $^{67}\text{Ga}$  and 18 MBq  $^{89}\text{Zr}$ . The labelled 7D12 (300  $\mu\text{g}$ ) was incubated at 37°C in a  $\text{CO}_2$ -enriched atmosphere (5%  $\text{CO}_2$ ) with freshly prepared human serum (1:4) in the presence of 0.02%  $\text{NaN}_3$ . Aliquots were taken after 5 and 24 h storage and analysed by ITLC and HPLC.

#### Biodistribution study

The distribution of  $^{68}\text{Ga}$ -Df-Bz-NCS-7D12 was examined using nude mice (Hsd:ATHymic Nude-*Foxn1*<sup>tm</sup>, 20–30 g, Harlan Laboratories, Horst, the Netherlands) bearing subcutaneously implanted human xenografts of the vulvar tumour cell line A431 at two lateral sides. All animal experiments were done according to NIH Principles of Laboratory Animal Care and Dutch national law (*Wet op de dierproeven*, Stb 1985, 336).

In this experiment mice bearing A431 xenografts were injected with 0.35 MBq  $^{68}\text{Ga}$ -Df-Bz-NCS-7D12 (6  $\mu\text{g}$ )

via the retro-orbital plexus. As reference compound, 0.35 MBq  $^{89}\text{Zr}$ -Df-Bz-NCS-7D12 (6  $\mu\text{g}$ ) was used. Unlabelled 7D12 was added to the injection mixture to obtain a final dose of 50  $\mu\text{g}$  per mouse. At 1, 2 and 3 h post-injection (p.i.) four mice were anaesthetized, bled, killed and dissected. Blood, tumour and normal tissues were weighed and radioactivity was measured in a gamma counter (Wallac, Turku, Finland). Radioactivity uptake for each sample was calculated as %ID/g.

#### PET study

PET imaging was performed on a HRRT PET scanner (Siemens/CTI [31]), a dedicated human brain scanner. Three A431 xenograft-bearing mice were anaesthetized by inhalation of 2% isoflurane, injected with 5 MBq  $^{68}\text{Ga}$ -Df-Bz-NCS-7D12 (85  $\mu\text{g}$ ) via the retro-orbital plexus and scanned for 3 h. In addition, three mice were injected with 2.5 MBq  $^{89}\text{Zr}$ -Df-Bz-NCS-7D12 (85  $\mu\text{g}$ ). Unlabelled 7D12 was added to the injection mixture to obtain a final dose of 100  $\mu\text{g}$  per mouse. Transmission scans for attenuation and scatter correction were routinely obtained with each emission scan. Three-dimensional emission scans were acquired in list mode during 180 min. A single frame static image was reconstructed using ordinary Poisson ordered subsets expectation maximization (OP-OSEM). For visualization of the images, the freely available Amide's A Medical Imaging Data Examiner (AMIDE) program was used [32].

#### Statistical analysis

Differences in tissue uptake between injected conjugates were statistically analysed for each different time point with SPSS 15.0 software using Student's *t* test for unpaired data. Two-sided significance levels were calculated and  $p < 0.01$  was considered statistically significant.

## Results

#### Preparation of $^{68/67}\text{Ga}$ -Df-Bz-NCS-cmAb U36

The Ga-Df formation conditions were investigated by performing experiments with premodified Df-Bz-NCS-cmAb U36. The Df-Bz-NCS chelate was coupled at pH 9 to the lysine groups in a threefold molar excess via a 30-min incubation at 37°C.

When labelling was performed for 5 min in a 2 ml acetate solution at a pH in the range of 5.0–6.5 and an activity level of 200 MBq  $^{68}\text{Ga}$  (2 pmol) and 37 MBq  $^{67}\text{Ga}$  (25 pmol), the labelling yield was consistently >90% provided the amount of mAb was >200  $\mu\text{g}$  (measured up

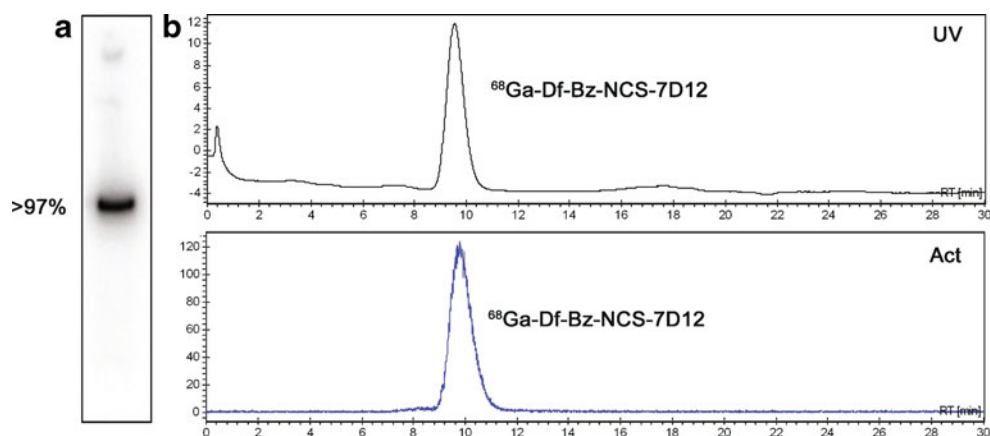
to 1,000  $\mu\text{g}$ ), i.e.  $>0.7$  nmol bound Df-groups. For 100  $\mu\text{g}$  (i.e. 0.35 nmol bound Df-groups) a labelling yield of 80% was obtained. When using a naked cmAb U36 under these conditions,  $< 1\%$  of Ga was co-eluted with the PD-10 protein fraction.

After PD-10 purification the labelled cmAb U36 was stored in 2 ml 0.25 M NaOAc with 5 mg ml<sup>-1</sup> gentisic acid, pH 5.5, and analysed. The radiochemical purity was always 96–99%, as determined with ITLC and HPLC. The immunoreactive fraction was determined by an overnight immunoreactivity assay (when using <sup>67</sup>Ga) and was 81–86%. The integrity of the labelled cmAb U36 was optimal as determined with SDS-PAGE and HPLC analysis (data not shown). The radiation dose derived from labelling with 200 MBq <sup>68</sup>Ga and its subsequent full decay did not affect the integrity and immunoreactivity of the <sup>68/67</sup>Ga product, which means that our chosen 0.25 M NaOAc with 5 mg ml<sup>-1</sup> gentisic acid, pH 5.5 buffer protected adequately against radiation damage. Dilution of the <sup>68/67</sup>Ga-cmAb U36 product with human serum to a solution containing 70 pmol/ml Df showed  $<1\%$  loss of label. Upon storage of this solution at 37°C, the radiochemical purity of cmAb U36 decreased during 5 h an additional 2% and during 24 h an additional 10%, as determined by ITLC and confirmed with HPLC.

#### Preparation of <sup>68/67</sup>Ga-Df-Bz-NCS-7D12 and <sup>89</sup>Zr-Df-Bz-NCS-7D12

The aforementioned conditions applied to Nanobody 7D12 gave 0.2 desferal groups per Nanobody molecule. Labelling (200–1,000  $\mu\text{g}$ ) of the Df-Bz-NCS-7D12 with <sup>68/67</sup>Ga resulted in overall radioactivity yields of 55–70% (not corrected for decay). Radiochemical purity was always 96–99%, as determined by HPLC and ITLC. Immunoreactivity was 40–60% for the 3-h incubation assay at 37°C while the overnight assay at 4°C using <sup>67</sup>Ga showed 80–85%. The integrity of the Nanobody was preserved as determined with SDS-PAGE and HPLC analysis (see Fig. 2).

**Fig. 2** SDS-PAGE followed by phosphor imaging analysis (a) and HPLC chromatogram (b) of purified <sup>68</sup>Ga-Df-Bz-NCS-7D12, where the upper panel represents the UV profile at 280 nm and the lower panel the radioactivity profile



For the <sup>89</sup>Zr-Df-Bz-NCS-7D12 the overall radioactivity yield was 59–73%, radiochemical purity was always 97–99% and the immunoreactivity was 80–85% (determined with the overnight assay at 4°C).

#### In vitro stability

In vitro stability of <sup>68/67</sup>Ga-Df-Bz-NCS-7D12 was compared with <sup>89</sup>Zr-Df-Bz-NCS-7D12. Radiochemical purity of <sup>68/67</sup>Ga-Df-Bz-NCS-7D12 was 98±1% at the start and only slightly decreased during 5 h incubation in buffer at 4°C (1.5–2.0% release of <sup>68/67</sup>Ga); after 24 h the decrease was 6–7% as determined with ITLC and confirmed with HPLC. For <sup>89</sup>Zr-Df-Bz-NCS-7D12 the radiochemical purity was also 98±1% at the start, which decreased to 97±1% after 24 h at 4°C. The integrity of both labelled 7D12 Nanobodies was not affected after 24 h at 4°C, as determined with SDS-PAGE and HPLC.

In human serum at 37°C, radiochemical purity of both labelled 7D12 Nanobodies slightly decreased during 5 h in human serum (1–2% release for both compounds), and after 24 h the percentage of <sup>68/67</sup>Ga that was dissociated was 7–8% and 1–2% for <sup>89</sup>Zr as determined by ITLC and confirmed with HPLC.

#### Biodistribution study

For the biodistribution study nude mice bearing A431 xenografts were injected with either 0.35±0.05 MBq <sup>68</sup>Ga-Df-Bz-NCS-7D12 or 0.35±0.01 MBq <sup>89</sup>Zr-Df-Bz-NCS-7D12 as the control group (Fig. 3). After 1 h high uptake was seen in tumour tissue for both radioisotopes (6.1±1.3% ID/g for <sup>68</sup>Ga and 7.5±1.9% ID/g for <sup>89</sup>Zr), a level which remained constant up to 3 h p.i. (6.1±0.9 and 7.6±1.9% ID/g at 2 h, and 7.2±1.5 and 7.4±1.6% ID/g at 3 h p.i. for <sup>68</sup>Ga and <sup>89</sup>Zr, respectively). High radioactivity uptake was found in the kidneys, urine and bladder. Except for some liver uptake (2.1±0.1 and 0.7±0.1% ID/g at 1 h p.i. for <sup>68</sup>Ga and <sup>89</sup>Zr, respectively) all other organs showed low uptake

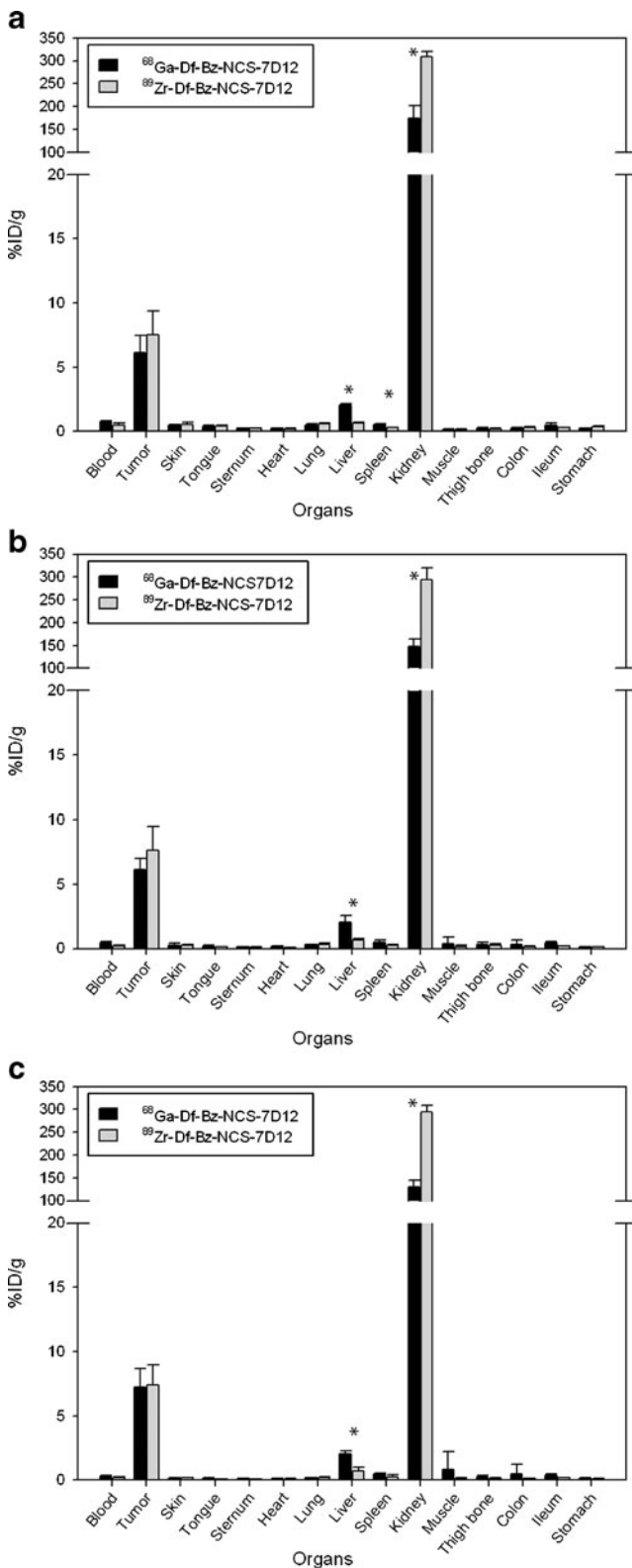


**Fig. 3** Biodistribution of 7D12 labelled with  $^{68}\text{Ga}$  (black bars) or  $^{89}\text{Zr}$  (grey bars) in A431 tumour-bearing nude mice at 1 h (a), 2 h (b) and 3 h (c) p.i. Significant differences in uptake are marked with an asterisk. Data are presented as average of four mice and standard deviation

at all time points ( $< 0.5 \pm 0.2\% \text{ID/g}$  for  $^{68}\text{Ga}$  and  $< 0.3 \pm 0.1\% \text{ID/g}$  for  $^{89}\text{Zr}$ ). For both radioisotopes tumour to blood ratios increased at later time points. At 1 h the tumour to blood ratio for  $^{68}\text{Ga}$  was 8.2 and increased to 14.4 at 2 h and 25.7 at 3 h p.i., while the tumour to blood ratios for  $^{89}\text{Zr}$  were 14.8, 35.2 and 42.4 at 1, 2 and 3 h, respectively. In general, the overall biodistribution of both radioisotopes was very similar. For all time points significant differences between  $^{68}\text{Ga}$  and  $^{89}\text{Zr}$  were seen in liver and kidney, and at 1 h p.i. a significant difference was also observed for spleen ( $p < 0.001$ ).

#### PET study

To exclude possible radioactivity uptake in non-evaluated tissues in the biodistribution studies a PET imaging study was performed. In Fig. 4 representative PET images are shown; a static PET image obtained 2–3 h after injection of  $^{68}\text{Ga}$ -Df-Bz-NCS-7D12 is seen in the left image while the right image represents a mouse 2–3 h after injection of  $^{89}\text{Zr}$ -Df-Bz-NCS-Df. In both images the tumours are clearly visible, with good tumour to background contrast. High accumulation in the kidney and bladder was observed.

#### Discussion

In this study, we describe a method for labelling of  $\alpha\text{EFGR}$  Nanobody 7D12 with  $^{68}\text{Ga}$  using the novel bifunctional desferal chelate (Df-Bz-NCS) which was previously introduced for the coupling of  $^{89}\text{Zr}$  to intact mAbs [22, 23]. Using this method, stable  $^{68}\text{Ga}$ -7D12 radioimmunoconjugates were produced as demonstrated by stability testing in storage buffer as well as in human serum with only slightly less stability as compared with the reference compound  $^{89}\text{Zr}$ -Df-Bz-NCS-7D12. In addition, high and selective tumour uptake was observed in biodistribution and PET imaging experiments in nude mice bearing A431 xenografts, which was similar for  $^{68}\text{Ga}$ -7D12 and the reference conjugate  $^{89}\text{Zr}$ -7D12. The latter indicates that Df-Bz-NCS is equally well suited for immuno-PET imaging, irrespective of whether the short-lived positron emitter  $^{68}\text{Ga}$  or the long-lived positron emitter  $^{89}\text{Zr}$  is used.  $^{89}\text{Zr}$ -Df antibodies have been extensively evaluated in clinical immuno-PET studies [33].

Crucial in the labelling procedures described herein are (1) the use of ultra pure HCl, to keep the  $^{nat}\text{Ga}$  concentrations as low as possible and also to minimize the amounts of Al, Fe and Zr, being strong competitors for complexation with Df, (2) the purification and concentration of  $^{68}\text{Ga}$  by use of an anion exchange column, to further minimize the amounts of Al, Fe and Zr, to get rid of contaminating metals originating from the generator and to

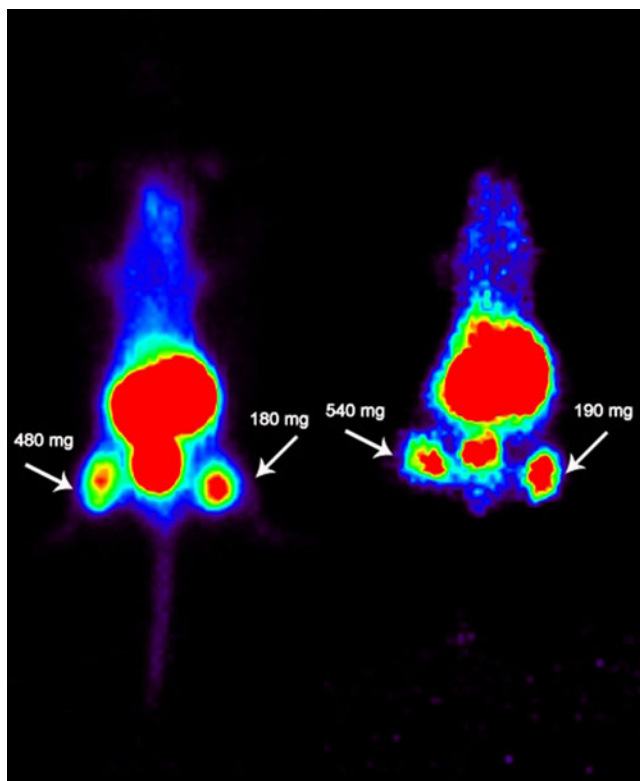


**Fig. 4** Static PET image of A431 tumour-bearing mice obtained 2–3 h after injection of  $^{68}\text{Ga}$ -Df-Bz-NCS-7D12 (*left mouse*) or  $^{89}\text{Zr}$ -Df-Bz-NCS-7D12 (*right mouse*). Images demonstrate similar uptake of both tracers. Tumours are indicated by *arrows*. Image planes have been chosen where both tumours were visible

keep  $[\text{}^{68}\text{GaCl}_4^-]$  volumes for labelling small [16, 34], (3) the addition of a highly concentrated  $\text{NH}_4\text{OAc}$  solution to the  $[\text{}^{68}\text{GaCl}_4^-]$  solution for efficient radiolabelling and stable complex formation (avoidance of the formation of gallium-oxo-chloro intermediates), (4) the use of a commercially available desferrioxamine B chelate that has been applied safely in the clinical setting for many years [23], (5) radiolabelling at room temperature within a relatively wide pH range of 5.0–6.5 and (6) the use of 0.25 M NaOAc with  $5\text{ mg ml}^{-1}$  gentisic acid, pH 5.5 for protection during storage of the purified  $^{68}\text{Ga}$ -labelled conjugate. These procedures appeared efficient and mild, thus avoiding denaturation of protein, and resulted in optimal quality conjugates at an overall radiochemical yield of 55–70% (not corrected for decay). Therefore, these generic procedures seem suitable for GMP-compliant labelling, irrespective of the intrinsic stability of the biomolecule.

The only chelate that has been used for  $^{68}\text{Ga}$  labelling of mAbs or mAb-like molecules for clinical purposes is DOTA [35]. With DOTA the best labelling kinetics were obtained in sodium acetate buffers at low pH [36]. Tolmachev et al. evaluated the  $^{68}\text{Ga}$  labelling kinetics of the DOTA-containing anti-HER2 Affibody ABY-002. La-

bellung at room temperature for 5 min appeared inefficient (decay-corrected yield of less than 5%). Only after elevation of the temperature to  $60^\circ\text{C}$  or  $90^\circ\text{C}$  did the yield increase to  $\sim 30\%$  and  $\sim 90\%$ , respectively. The binding and pharmacokinetic characteristics of this particular Affibody did not become affected upon labelling, but it is open to question whether other proteins can resist the harsh labelling conditions of low pH and high temperature [35, 37]. The same is true for microwave heating that has been used for labelling of DOTA bioconjugates with  $^{68}\text{Ga}$  [16, 38]. In our initial studies, using DOTA-Bz-NCS, less than 60% labelling was obtained after 20 min at  $45^\circ\text{C}$ , while the thus obtained labelled product was unstable. We postulate that at lower temperature no full N-coordination occurs. This means that the  $^{68}\text{Ga}$  atom becomes ligated to the carboxyl functions of the DOTA molecule with still having water molecules in its coordination sphere instead of N, and that only concordant heating at elevated temperatures [37, 39] creates the additional N-coordination of the DOTA molecule leading to the  $^{68}\text{Ga}$ -DOTA complex that is suitable for in vivo applications. This important aspect of complex formation is fully analogous to what has been shown by us for the synthesis of the  $^{186}\text{Re}$ -MAG3 complex [40].

NOTA and its derivatives as well as the recently introduced HBED-CC chelates might have advantages over DOTA, since labelling with these chelates can be performed at room temperature and modest pH [19–21, 41]. These chelates, however, have not been clinically evaluated yet, and for us this was the reason to evaluate the desferrioxamine B derivative. Some controversy exists about the conditional stability constant of the Ga-Df complex at neutral pH. The in vitro stability we found corresponds well with the earlier findings of Smith-Jones et al. [25], Fani et al. [27] and Furukawa et al. [24], but seems to be rather in contrast with the findings of Caraco et al. [42] and Govindan et al. [26]. We feel that this is only an apparent controversy because the conditions under which Caraco et al. produced their Ga-Df complex are completely different. We observed that a product formed at pH=7.4 indeed suffered from instability indicating that at this pH a certain amount of weak complexes are formed containing partly hydrolyzed Ga ions and so being only mono- or bidentate bound to the three hydroxamate functions. With respect to the findings of Govindan et al. [26], they already suggested themselves that their findings are most probably mixed up by the fact that the linkages between their mAb and Df are intrinsically instable.

EGFR, a tyrosine kinase receptor, is highly expressed in many epithelial cancer cells and is a prime target for detection and therapeutic applications. Nuclear imaging techniques have a proven advantage over immunohistological techniques since nuclear imaging is noninvasive and whole-body scans



can be obtained [43]. The use of Nanobodies as imaging moiety might have advantages over the use of intact mAbs, since a molecular weight of only 15 kDa allows for faster kinetics than intact mAbs *in vivo*. To our knowledge, Nanobodies have never been used for immuno-PET applications. In this study,  $^{68}\text{Ga}$ -labelled Nanobody 7D12 showed high and selective uptake in A431 tumours, ranging from 6.1 to 7.2%ID/g at 1–3 h p.i., which was comparable to the reference compound  $^{89}\text{Zr}$ -7D12 (7.5 to 7.4%ID/g at 1–3 h). Significant differences in liver and kidney uptake were observed between the  $^{68}\text{Ga}$ -7D12 and  $^{89}\text{Zr}$ -7D12 conjugates. These differences most probably reflect the slightly lower stability observed in the *in vitro* stability experiments. Maybe metabolite analyses might provide further insight.

Huang et al. [44] and Gainkam et al. [45] studied the same ( $\alpha\text{EGFR}$ ) Nanobody 7D12 in the same A431 xenograft model, but labelled with  $^{99\text{m}}\text{Tc}$  for SPECT applications. Tumour uptake of  $^{99\text{m}}\text{Tc}$ -7D12 was 4.9%ID/g at 1 h p.i. (assessed by quantitative analysis of SPECT images) and 6.1%ID/g at 1.5 h p.i. (assessed by radioactivity counting of dissected tumours). Like  $^{68}\text{Ga}$ -7D12,  $^{99\text{m}}\text{Tc}$ -7D12 showed high kidney uptake. However, uptake of  $^{99\text{m}}\text{Tc}$ -7D12 in lung and spleen was higher than that of  $^{68}\text{Ga}$ -7D12: 2.1 and 1.4% ID/g versus 0.5 and 0.6%ID/g at 1 h p.i. Given the superior properties of PET in comparison to SPECT for clinical quantitative imaging, these data suggest that  $^{68}\text{Ga}$ -7D12 is the more attractive Nanobody-based probe for assessment of EGFR expression [46, 47].

$^{68}\text{Ga}$ -7D12 allowed high contrast imaging at relatively early time points (1 h p.i.) in comparison with radiolabelled conventional intact mAbs used in other preclinical imaging studies. For example, in recent immuno-PET studies with  $^{64}\text{Cu}$ - and  $^{89}\text{Zr}$ -labelled anti-EGFR mAb cetuximab tumours could only be clearly delineated 16–24 h p.i. [7, 9, 48]. Another interesting small molecular protein was introduced for imaging of EGFR, namely the 8-kDa Affibody  $Z_{\text{EGFR}:2377}$  [49]. PET imaging studies in A431-bearing nude mice showed higher tumour contrast when 50  $\mu\text{g}$  of  $^{111}\text{In}$ -labelled  $Z_{\text{EGFR}:2377}$  was injected in comparison to 5  $\mu\text{g}$ , whereas for both doses high liver uptake was observed. For the 50  $\mu\text{g}$   $^{111}\text{In}$ - $Z_{\text{EGFR}:2377}$  group, tumour and liver uptake at 4 h p.i. was 2.4 and 5.1%ID/g, respectively. In comparison, tumour uptake of  $^{68}\text{Ga}$ -7D12 in the present study was substantially higher (7.2%ID/g at 3 h p.i.), while liver uptake was lower (2.0%ID/g at 3 h p.i.). These interesting differences in uptake can be ascribed to differences in reactivity with murine EGFR. Both probes can bind to human EGFR expressed in human xenografts, but only  $^{111}\text{In}$ - $Z_{\text{EGFR}:2377}$  can also bind to the murine EGFR in the liver. In accordance, initial clinical imaging studies with  $^{111}\text{In}$ -labelled anti-EGFR mAb 225 showed high liver uptake, requiring relatively high mAb doses for imaging of EGFR expression [50].

The aforementioned data indicate  $^{68}\text{Ga}$ -7D12 Nanobody has potential for assessment of EGFR tumour expression; however, for clinical application thorough dose optimization might be needed to obtain optimal imaging results. The latter will be easier for  $^{68}\text{Ga}$ -labelled Nanobodies directed against targets that show predominantly expression in the tumour, as was recently illustrated in PET imaging studies with  $^{68}\text{Ga}$ -labelled Affibody ABY-002 directed against the HER2 receptor [35].

## Conclusion

The newly developed GMP-compliant two-step procedure for coupling desferal to a Nanobody allows efficient and rapid preparation of  $^{68}\text{Ga}$ -Nanobodies for clinical use with high labelling yields, high radiochemical purity and preservation of immunoreactivity. The anti-EGFR  $^{68}\text{Ga}$ -Df-Bz-NCS-7D12 Nanobody showed high accumulation in A431 xenografts in nude mice in biodistribution studies as well as in immuno-PET, which indicates that this conjugate can be a promising fast kinetic noninvasive imaging probe for the detection of EGFR expression in tumours.

**Acknowledgements** This project was financially supported by the Dutch Technology Foundation (STW, grant 10074) and partly performed within the framework of CTMM, the Center for Translational Molecular Medicine ([www.ctmm.nl](http://www.ctmm.nl)), project AIRFORCE number 030-103. The authors thank Leo van Rooij and Peter Schollemma of the radionuclide center for their assistance with the  $^{68}\text{Ga}/^{68}\text{Ge}$  generator and Marc Huisman for PET analysis.

**Conflicts of interest** None.

**Open Access** This article is distributed under the terms of the Creative Commons Attribution Noncommercial License which permits any noncommercial use, distribution, and reproduction in any medium, provided the original author(s) and source are credited.

## References

1. Yarden Y, Sliwkowski MX. Untangling the ErbB signalling network. *Nat Rev Mol Cell Biol* 2001;2:127–37.
2. Lurje G, Lenz HJ. EGFR signaling and drug discovery. *Oncology* 2009;77:400–10.
3. Dadparvar S, Krishna L, Miyamoto C, Brady LW, Brown SJ, Bender H, et al. Indium-111-labeled anti-EGFr-425 scintigraphy in the detection of malignant gliomas. *Cancer* 1994;73:884–9.
4. Vallis KA, Reilly RM, Chen P, Oza A, Hendler A, Cameron R, et al. A phase I study of  $^{99\text{m}}\text{Tc}$ -hR3 (DiaCIM), a humanized immunoconjugate directed towards the epidermal growth factor receptor. *Nucl Med Commun* 2002;23:1155–64.
5. Schechter NR, Wendt RE, Yang DJ, Azhdarinia A, Erwin WD, Stachowiak AM, et al. Radiation dosimetry of  $^{99\text{m}}\text{Tc}$ -labeled C225 in patients with squamous cell carcinoma of the head and neck. *J Nucl Med* 2004;45:1683–7.

6. Niu G, Li Z, Xie J, Le QT, Chen X. PET of EGFR antibody distribution in head and neck squamous cell carcinoma models. *J Nucl Med* 2009;50:1116–23.
7. Cai W, Chen K, He L, Cao Q, Koong A, Chen X. Quantitative PET of EGFR expression in xenograft-bearing mice using <sup>64</sup>Cu-labeled cetuximab, a chimeric anti-EGFR monoclonal antibody. *Eur J Nucl Med Mol Imaging* 2007;34:850–8.
8. Ping Li W, Meyer LA, Capretto DA, Sherman CD, Anderson CJ. Receptor-binding, biodistribution, and metabolism studies of <sup>64</sup>Cu-DOTA-cetuximab, a PET-imaging agent for epidermal growth-factor receptor-positive tumors. *Cancer Biother Radiopharm* 2008;23:158–71.
9. Aerts HJ, Dubois L, Perk L, Vermaelen P, van Dongen GA, Wouters BG, et al. Disparity between in vivo EGFR expression and <sup>89</sup>Zr-labeled cetuximab uptake assessed with PET. *J Nucl Med* 2009;50:123–31.
10. Roovers RC, van Dongen GA, van Bergen en Henegouwen PM. Nanobodies in therapeutic applications. *Curr Opin Mol Ther* 2007;9:327–35.
11. Tijink BM, Laeremans T, Budde M, Stigter-van Walsum M, Dreier T, de Haard HJ, et al. Improved tumor targeting of anti-epidermal growth factor receptor Nanobodies through albumin binding: taking advantage of modular Nanobody technology. *Mol Cancer Ther* 2008;7:2288–97.
12. Kolkman JA, Law DA. Nanobodies – from llamas to therapeutic proteins. *Drug Discov Today: Technol* 2010. doi: 10.1016/j.ddtec.2010.03.002.
13. Hamers-Casterman C, Atarhouch T, Muyldermans S, Robinson G, Hamers C, Songa EB, et al. Naturally occurring antibodies devoid of light chains. *Nature* 1993;363:446–8.
14. Roovers RC, Laeremans T, Huang L, De Taeye S, Verkleij AJ, Revets H, et al. Efficient inhibition of EGFR signaling and of tumour growth by antagonistic anti-EFGR Nanobodies. *Cancer Immunol Immunother* 2007;56:303–17.
15. Els Conrath K, Lauwereys M, Wyns L, Muyldermans S. Camel single-domain antibodies as modular building units in bispecific and bivalent antibody constructs. *J Biol Chem* 2001;276:7346–50.
16. Velikyan I, Beyer GJ, Långström B. Microwave-supported preparation of (68)Ga bioconjugates with high specific radioactivity. *Bioconjug Chem* 2004;15:554–60.
17. Hoffend J, Mier W, Schuhmacher J, Schmidt K, Mitropoulou-Strauss A, Strauss LG, et al. Gallium-68-DOTA-albumin as a PET blood-pool marker: experimental evaluation in vivo. *Nucl Med Biol* 2005;32:287–92.
18. Blom E, Långström B, Velikyan I. <sup>68</sup>Ga-labeling of biotin analogues and their characterization. *Bioconjug Chem* 2009;20:1146–51.
19. Ferreira CL, Lamsa E, Woods M, Duan Y, Fernando P, Bensimon C, et al. Evaluation of bifunctional chelates for the development of gallium-based radiopharmaceuticals. *Bioconjug Chem* 2010;21:531–6.
20. Eder M, Wangler B, Knackmuss S, LeGall F, Little M, Haberkorn U, et al. Tetrafluorophenolate of HBED-CC: a versatile conjugation agent for <sup>68</sup>Ga-labeled small recombinant antibodies. *Eur J Nucl Med Mol Imaging* 2008;35:1878–86.
21. Eder M, Knackmuss S, Le Gall F, Reusch U, Rybin V, Little M, et al. (68)Ga-labelled recombinant antibody variants for immuno-PET imaging of solid tumours. *Eur J Nucl Med Mol Imaging* 2010;37:1397–407.
22. Perk LR, Vosjan MJ, Visser GW, Budde M, Jurek P, Kiefer GE, et al. p-Isothiocyanatobenzyl-desferrioxamine: a new bifunctional chelate for facile radiolabeling of monoclonal antibodies with zirconium-89 for immuno-PET imaging. *Eur J Nucl Med Mol Imaging* 2009;37:250–9.
23. Vosjan MJ, Perk LR, Visser GW, Budde M, Jurek P, Kiefer GE, et al. Conjugation and radiolabeling of monoclonal antibodies with zirconium-89 for PET imaging using the bifunctional chelate p-isothiocyanatobenzyl-desferrioxamine. *Nat Protoc* 2010;5:739–43.
24. Furukawa T, Fujibayashi Y, Fukunaga M, Saga T, Endo K, Yokoyama A. An approach for immunoradiometric assay with metallic radionuclides: gallium-67-deferoxamine-dialdehyde starch-IgG. *J Nucl Med* 1991;32:825–9.
25. Smith-Jones PM, Stolz B, Bruns C, Albert R, Reist HW, Fridrich R, et al. Gallium-67/gallium-68-[DFO]-octreotide—a potential radiopharmaceutical for PET imaging of somatostatin receptor-positive tumors: synthesis and radiolabeling in vitro and preliminary in vivo studies. *J Nucl Med* 1994;35:317–25.
26. Govindan SV, Michel RB, Griffiths GL, Goldenberg DM, Mattes MJ. Deferoxamine as a chelator for <sup>67</sup>Ga in the preparation of antibody conjugates. *Nucl Med Biol* 2005;32:513–9.
27. Fani M, André JP, Maecke HR. <sup>68</sup>Ga-PET: a powerful generator-based alternative to cyclotron-based PET radiopharmaceuticals. *Contrast Media Mol Imaging* 2008;3:67–77.
28. Schrijvers AH, Quak JJ, Uyterlinde AM, van Walsum M, Meijer CJ, Snow GB, et al. MAb U36, a novel monoclonal antibody successful in immunotargeting of squamous cell carcinoma of the head and neck. *Cancer Res* 1993;53:4383–90.
29. Welters MJ, Fichtinger-Schepman AM, Baan RA, Hermsen MA, van der Vijgh WJ, Cloos J, et al. Relationship between the parameters cellular differentiation, doubling time and platinum accumulation and cisplatin sensitivity in a panel of head and neck cancer cell lines. *Int J Cancer* 1997;71:410–5.
30. Lindmo T, Boven E, Cuttitta F, Fedorko J, Bunn PA. Determination of the immunoreactive fraction of radiolabeled monoclonal antibodies by linear extrapolation to binding at infinite antigen excess. *J Immunol Methods* 1984;72:77–89.
31. de Jong HW, van Velden FH, Kloet RW, Buijs FL, Boellaard R, Lammertsma AA. Performance evaluation of the ECAT HRRT: an LSO-LYSO double layer high resolution, high sensitivity scanner. *Phys Med Biol* 2007;52:1505–26.
32. Loening AM, Gambhir SS. AMIDE: a free software tool for multimodality medical image analysis. *Mol Imaging* 2003;2:131–7.
33. van Dongen GA, Vosjan MJ. Immuno-positron emission tomography: shedding light on clinical antibody therapy. *Cancer Biother Radiopharm* 2010;25:375–85.
34. Gebhardt P, Opfermann T, Saluz HP. Computer controlled <sup>68</sup>Ga milking and concentration system. *Appl Radiat Isot* 2010;68:1057–9.
35. Baum RP, Prasad V, Muller D, Schuchardt C, Orlova A, Wennborg A, et al. Molecular imaging of HER2-expressing malignant tumors in breast cancer patients using synthetic <sup>111</sup>In- or <sup>68</sup>Ga-labeled affibody molecules. *J Nucl Med* 2010;51:892–7.
36. Tolmachev V, Stone-Elander S. Radiolabelled proteins for positron emission tomography: pros and cons of labelling methods. *Biochim Biophys Acta* 2010;1800:487–510.
37. Tolmachev V, Velikyan I, Sandström M, Orlova A. A HER2-binding Affibody molecule labelled with (68)Ga for PET imaging: direct in vivo comparison with the (111)In-labelled analogue. *Eur J Nucl Med Mol Imaging* 2010;37:1356–67.
38. Velikyan I, Sundberg AL, Lindhe O, Höglund AU, Eriksson O, Werner E, et al. Preparation and evaluation of (68)Ga-DOTA-hEGF for visualization of EGFR expression in malignant tumors. *J Nucl Med* 2005;46(11):1881–8.
39. Ren G, Zhang R, Liu Z, Webster JM, Miao Z, Gambhir SS, et al. A 2-helix small protein labeled with <sup>68</sup>Ga for PET imaging of HER2 expression. *J Nucl Med* 2009;50:1492–9.
40. Visser GW, Gerretsen M, Herscheid JD, Snow GB, van Dongen G. Labeling of monoclonal antibodies with rhenium-186 using the MAG3 chelate for radioimmunotherapy of cancer: a technical protocol. *J Nucl Med* 1993;34:1953–63.
41. Riss PJ, Kroll C, Nagel V, Rösch F. NODAPA-OH and NODAPA-(NCS)n: synthesis, <sup>68</sup>Ga-radiolabelling and in vitro character-

- isation of novel versatile bifunctional chelators for molecular imaging. *Bioorg Med Chem Lett* 2008;18:5364–7.
42. Caraco C, Aloj L, Eckelman WC. The gallium-deferoxamine complex: stability with different deferoxamine concentrations and incubation conditions. *Appl Radiat Isot* 1998;49:1477–9.
  43. Weissleder R. Molecular imaging in cancer. *Science* 2006;312:1168–71.
  44. Huang L, Gainkam LO, Caveliers V, Vanhove C, Keyaerts M, De Baetseliens P, et al. SPECT imaging with (99m)Tc-labeled EGFR-specific Nanobody for in vivo monitoring of EGFR expression. *Mol Imaging Biol* 2008;10:167–75.
  45. Gainkam LO, Huang L, Caveliers V, Keyaerts M, Hemot S, Vaneycken I, et al. Comparison of the biodistribution and tumor targeting of two 99mTc-labeled anti-EGFR Nanobodies in mice, using pinhole SPECT/micro-CT. *J Nucl Med* 2008;49:788–95.
  46. Verel I, Visser GW, van Dongen GA. The promise of immuno-PET in radioimmunotherapy. *J Nucl Med* 2005;46 Suppl 1:164S–71.
  47. Börjesson PK, Jauw YW, de Bree R, Roos JC, Castelijns JA, Leemans CR, et al. Radiation dosimetry of 89Zr-labeled chimeric monoclonal antibody U36 as used for immuno-PET in head and neck cancer patients. *J Nucl Med* 2009;50:1828–36.
  48. Perk LR, Visser GW, Vosjan MJ, Stigter-van Walsum M, Tjink BM, Leemans CR, et al. (89)Zr as a PET surrogate radioisotope for scouting biodistribution of the therapeutic radiometals (90)Y and (177)Lu in tumor-bearing nude mice after coupling to the internalizing antibody cetuximab. *J Nucl Med* 2005;46:1898–906.
  49. Tolmachev V, Rosik D, Wällberg H, Sjöberg A, Sandström M, Hansson M, et al. Imaging of EGFR expression in murine xenografts using site-specifically labelled anti-EGFR 111In-DOTA-Z EGFR:2377 Affibody molecule: aspect of the injected tracer amount. *Eur J Nucl Med Mol Imaging* 2010;37:613–22.
  50. Divgi CR, Welt S, Kris M, Real FX, Yeh SD, Gralla R, et al. Phase I and imaging trial of indium 111-labeled anti-epidermal growth factor receptor monoclonal antibody 225 in patients with squamous cell lung carcinoma. *J Natl Cancer Inst* 1991;83:97–104.